Exfoliated carbon nitrides for corrosion prevention in radiators: temperature-dependent corrosion analysis

D. Vasudevan*, A. Kumaravel, A. Murugesan, A. Mugil, B. Karthi, K. K. Kumar
Department of Mechanical Engineering, K.S. Rangasamy College of Technology, Tiruchengode – 637 215, Tamil Nadu, India

This article outlines the preparation and exfoliation of graphitic-carbon nitride (GCN) by thermal polymerization technique using urea proceeded by the hydrothermal approach for the application of corrosion resistance in radiators. The prepared sample was characterized by using various methods. X-ray powder diffraction (XRD) and Fourier-transform infrared spectroscopy (FT-IR) confirmed the purity of GCN, and Surface morphology results revealed the formation of spherical-shaped GCN. Herein, graphitic carbon nitride (GCN) was synthesized to enhance its corrosion-resistance performance on mild steel (MS) under a seawater atmosphere. The corrosion behaviour of the graphitic-carbon nitride (GCN) synthesized by the hydrothermal method was examined by conducting electrochemical corrosion tests in a 3.5% NaCl medium under three different temperatures. The excellent temperature dependant electro-catalytic activity of the prepared GCN was analysed. The hydrothermal exfoliation process highly enhances the structural, optical, and electrochemical properties like corrosion resistance and stability of the prepared GCN. This study demonstrates that hydrothermally exfoliated GCN exhibits low corrosion rates and high electrochemical corrosion resistance, which could be a potential candidate for corrosion inhibitors in radiators.

(Received March 20, 2023; Accepted August 11, 2023)

Keywords: Urea, Graphitic carbon nitrate, Corrosion resistance, Radiators

1. Introduction

Metal corrosion is a process that has significant economic consequences on modern industrial civilization and poses a severe risk to human health and the environment. Many initiatives are made to understand and develop methods for preventing corrosion in metals. Consequently, corrosion cannot be prevented; thus, corrosion management is the only alternative for reducing the kinetics or altering the cause [1-3]. Surface corrosion is the progressive destruction of metal due to chemical interactions with environmental factors. Impurities and metal reactivity that may arise on metal surfaces are two factors that contribute to corrosion. Mild steel (MS) is widely utilized because of its high mechanical strength and affordable manufacture; it is employed in chemical and petrochemical engineering as a fabricating material and has a wide range of structural and mechanical uses in different sectors [4-5]. In order to achieve hydrogen evolution by aqua-organic liquid reforming, a variety of nanostructured oxide semiconductors, including simple and complex oxides, as well as oxide-based composites, were used as the catalyst. The bulk of these materials do, however, include d- and f-elements, which limits their economic use, mandate their recovery, and create environmental problems when disposed of. Thus, a vital and active area of modern solid physics, chemistry, and materials research is the search for new metal-free compounds with high catalytic activity. [6-8].

Non-metallic semiconducting materials have similar efficiency to metal oxide photocatalysts due to their minimal cost of materials and a corresponding region of light absorption. Polymeric graphitic carbon nitride (GCN) is a metal-free material widely explored in various applications. GCN is a polymeric semiconductor material featuring a graphene-like structure. Graphene comprises primarily carbon (C), whereas GCN includes carbon and nitrogen (N). It is related to graphite and belongs to carbon nitrides, which have atoms with excellent

* Corresponding author: vasudevan.vi@gmail.com
https://doi.org/10.15251/DJNB.2023.183.985

covalent bonding. Due to the presence of the tri-s-triazine and heptazine rings, GCN is thought to be the most stable allotrope of carbon nitride. They also include tri-s-triazine units, which are chemically stable under both acidic and alkaline environments and have high heat constancy. These units have a planar layer with a π-conjugated arrangement. The weak van der Waals force between the various layers and the great condensation ability of the tri-s-triazine rings (30 kJ mol 1) make this an indirect semiconductor with excellent photocatalytic and electro-catalytic capabilities [9-11]. Many techniques have been developed to produce GCN nitrogen-rich by heat polymerization. Thus, the organic template is crucial in emerging a porous structure. Notwithstanding its advantages, the low surface area and poor dispersion nature of bulk GCN limit its effectiveness in electrochemical functions [12]. However, the unique surface area, adsorption capacity, and electron transfer efficiency of bulk GCN may be enhanced by exfoliation. Exfoliation of GCN has been performed using various approaches, where, herein, we synthesized simple and effective exfoliation using the hydrothermal method [13].

Radiator materials are most often made of mild steel. In fact, mild steel is so widely used that it's likely that every radiator you've ever seen is constructed of it. This is due to a variety of factors. First off, mild steel radiators are inexpensive to create, making them inexpensive for you to purchase [4-6]. Radiator corrosion, an all-too-common cooling system failure, is most likely the source of this issue, but there may be other elements at play as well. A radiator may get corroded over time and is often quite obvious, although other forms of corrosion are more difficult to anticipate. It's critical to keep an eye out for corrosion damage to prevent expensive repairs after it has begun. Radiator corrosion damage may result in decreased performance and cooling efficiency. Flimsy and fragile tubes, leaks or losses of coolant, sludge or debris accumulation (clogging), metal pitting, cracking, or general degradation, the blending of coolant and transmission fluid Overheating, radiator malfunction. So, the automotive industry's main challenge is to avoid corrosion in radiators. Mild steel, which is often used in radiators, may be improved in a number of ways. Using anticorrosive coolant in radiators is one of them. Materials made of carbon naturally have high levels of corrosion resistance [10-13].

Herein, we have prepared a hydrothermally exfoliated graphitic carbon nitride (H-GCN) for the anti-corrosion application using a simple hydrothermal method. Utilizing XRD, FTIR, and SEM investigation, the synthesized GCN was characterized, and its structural, absorption bands, and SEM micrographs were investigated. Electrochemical properties of GCN and H-GCN were carried out by LSV and EIS under 3.5% of NaCl electrolytes at three different electrolyte temperatures

2. Experimental

2.1. Materials

N-methyl-2-pyrrolidone, ethanol, polyvinylidene fluoride, urea (CH_4N_2O), and double-distilled water were all procured from Merck and used without extra purification. As an electrolyte, sodium chloride (NaCl) is used.

2.2. Preparation of exfoliated H-GCN

The bulk GCN was synthesized using thermal condensation polymerization of urea (Sigma Aldrich, India). Usually, 10 g of urea was heated for 4 hours at 550 °C in ambient air and held in a capped porcelain container in the muffle heater. The calcined material was permitted to cool to ambient temperature before being thoroughly ground into a light-yellow product. The finally collected powder was named GCN. The exfoliation of bulk GCN was carried out by the aqueous hydrothermal method. In the first step, 100 mL of distilled water was mixed with 0.5 g of bulk GCN nanopowder, and the mixture was agitated with a magnetic stirrer for 15 minutes. Then, the resulting white suspension was transferred hydrothermal Teflon beaker and heated for 6 hours at 150 °C. Finally, an extremely dry, H-GCN nanopowder was produced by drying the resulting colloidal solution at 100 °C until the water had been removed, followed by 30 minutes of annealing at 300 °C.

2.3. Sample preparation for corrosion studies

In order to evaluate the anticorrosive qualities of the synthesized GCN and H-GCN samples, linear sweep voltammetry and electrochemical impedance spectroscopy (EIS) were both used (LSV). 15 mg of prepared GCN and H-GCN samples were individually mixed with 80:15:5 weight ratios of polyvinylidene difluoride (PVDF) and N-methyl-2-pyrrolidone (NMP) to create a slurry. Using the doctor's blade technique, the slurry was also applied to the mild steel (MS) plate's surface. The coated plate was dried in a hot-air oven at 353K for an hour before being used as an electrolyte for corrosion experiments.

2.4. Characterization techniques

The crystal structure of the as-prepared sample was examined using XRD (XPERT-PRO, The Netherlands). Using an FTIR spectrophotometer, the existence of functional groups was investigated in the 4000-400 cm^{-1} FTIR range (Spectrum 100; PerkinElmer, USA). SEM was used to characterize the surface (JSM-6510). Equipment Autolab PGSTAT302N was used to conduct electrochemical measurements (Metrohm Autolab, The Netherlands). The voltammetry measurement is performed using a three-electrode setup with platinum wire serving as the reference electrode and the counter electrode, GCN, and modified GCN serving as the working electrode (1 cm^2).

2.5. Electrochemical studies

Using a three-electrode-cell arrangement, the corrosion-characteristic behavior in Mild steel (MS) plate was investigated. The specimens served as the working electrodes in this cell arrangement, with Ag/AgCl serving as the reference electrode and platinum serving as the counter electrode. Using the Autolab PGSTAT302N apparatus, electrochemical corrosion tests were performed on GCN and hydrothermally exfoliated GCN in 3.5% NaCl electrolyte under three different temperatures, i.e., 25 ℃, 50℃, and 75 ℃ (Metrohm Autolab, The Netherlands). At a scan rate of 1 mV/s, the applied potential window for corrosion tests was -2 to 0 V. Corrosion potential (Ecorr), and corrosion current was determined from the Tafel plot of the LSV test. The impedance measurements for GCN and hydrothermally exfoliated GCN were obtained using the frequency range of 0.01-100 kHz.

3. Results and discussion

3.1. X-Ray diffraction

The phase and purity of synthesized GCN and H-GCN were examined using XRD, and 2Θ angular region between 10˚and 80˚ was inspected and displayed in Figure 1. The two prominent diffraction peaks at 27.4˚ and 13.1˚ correlated well with the layered GCN diffraction planes (002) and (100). These data closely resemble the card number 87-1526 issued by the JCPDS [14]. The most substantial peak, at 27.4˚, was attributed to the aromatic system of interlayer stacking.

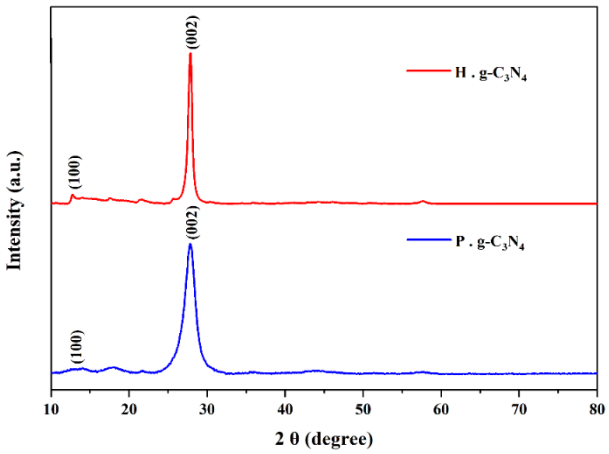

Fig. 1. XRD pattern of synthesized GCN and H-GCN.

This peak depicts the formation of GCN due to the thermal pyrolysis process' emission of ammonium gas. The smallest peak, at 13.1˚, was related to in-planar tris-s-triazine structural packing [15-16]. These findings suggested that the GCN film was successfully synthesized. H-GCN exhibits the same XRD pattern as bulk GCN exhibits. Comparing the GCN (002) peaks to those of H-GCN, there is a slight shift toward lower 2θ. The intensity somewhat reduced at the same time as the major diffraction plane (002) moved from 27.4 to 27.5. The change is more pronounced in H-GCN, which shows that interlayer stacking has weakened after the exfoliation and that the GCN interlayer distance has increased. Notably, no impurity peaks are seen.

The crystallite size is between 21.3 and 13.5 nm for GCN and H-GCN. Using the standard Debye-Scherrer equation, the following is derived for the average crystallite size [17].

3.2. FTIR analysis

FTIR spectra of synthesized GCN and H-GCN are shown in Figure 2. For bulk and H-GCN, the amino groups -NH and H2O were assigned the strong bond at 3250–3081 cm^{-1}. N-H stretching, which resembles urea's existence, is indicated by the band at 3200-3500 cm-1 [8]. The stretching vibration modes of carbon-nitrogen and carbon-hydrogen in the C-N heterocycles were ascribed to several peaks around the 1200–1600 cm^{-1} region observed in both GCN and H-GCN samples [16]. The repeating units of GCN exhibit these stretching modes of the CN heterocyclic bonds. The C=C stretching vibrations in the aromatic ring cause the peak to appear at a wavelength of 1636 cm^{-1}. The vibrations of s-triazine units are attributed to the peaks between 1800 and 900 cm^{-1} [19], whereas the peak at around 809 cm^{-1} was attributed to the vibrational bands of the triazine ring. The sharp band at near 812 cm^{-1} indicates the presence of a CN heterocycle during the thermal polymerization of pure urea [20]. Therefore, the XRD and FTIR data confirm the GCN formation.

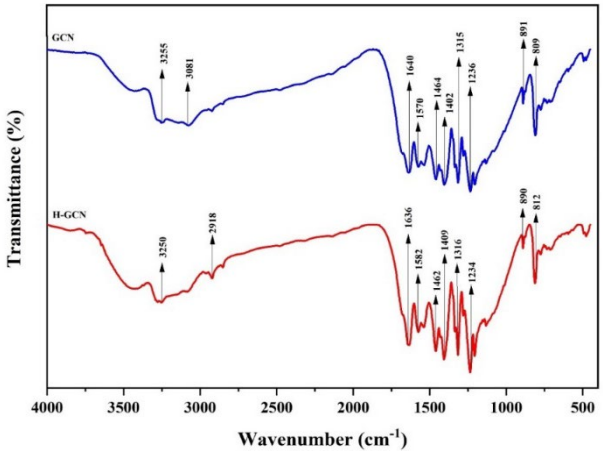

Fig. 2. FTIR images of GCN and H-GCN.

3.3. Morphology analysis

The Scanning electron microscope images of GCN and H-GCN SEM are represented in Figure 3. Figure 3 a) no deep fissures were seen in bulk GCN and Figure 3 b) shows the agglomerated and irregular spherical shape morphology observed in H-GCN. Graphitic carbon nitrides with both original and exfoliated graphite sheets exhibit GCN nanosheet agglomerates similar to crumpled paper sheets. The original sample exhibited tight sphere-like forms that were nearly eliminated after exfoliation. With increasing space between the GCN nanosheets, the material becomes more porous and looser. Graphitic carbon nitride agglomerates are exfoliated into individual nanosheets, as shown by X-ray diffractometry, causing a widening of the diffraction lines.

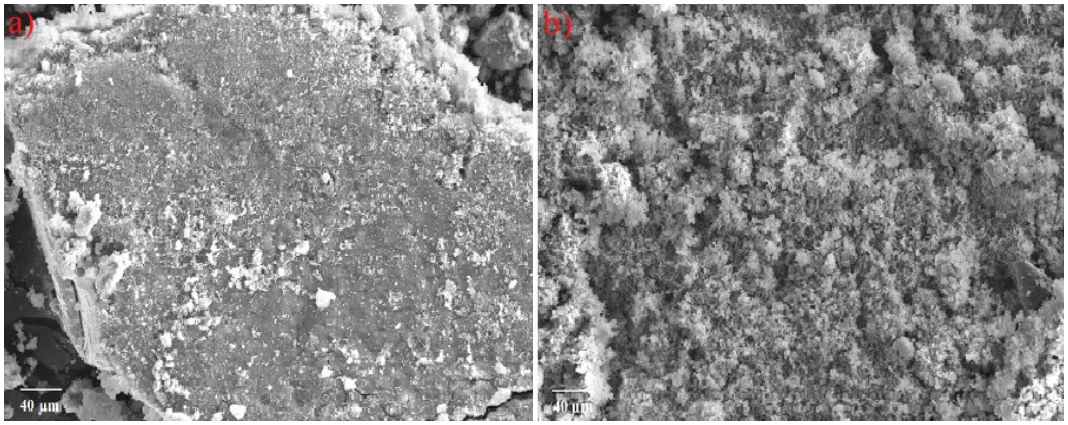

Fig. 3. SEM image of a) GCN and b) Exfoliated H-GCN.

3.4. Particle size analysis

Figure 4 displays the average particle size analyses for GCN and hydrothermally exfoliated GCN. As a result, the estimated (d_{50}) average particle sizes for both GCN and hydrothermally exfoliated GCN are 38.75 nm and 23.58 nm, respectively. When comparing GCN with H-GCN, the GCN's typical particle size remained more significant than the hydrothermally exfoliated GCN.

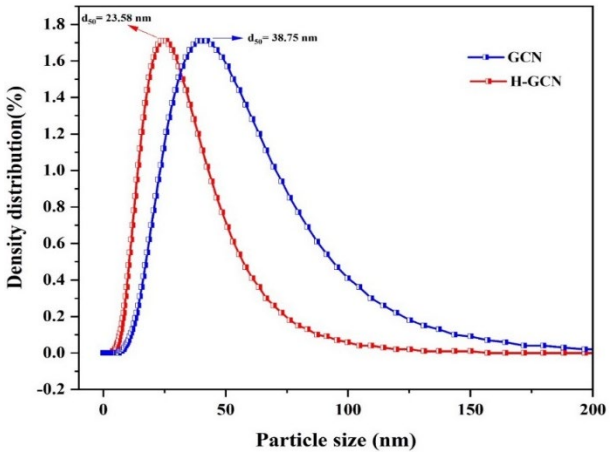

Fig. 4. PSA image of GCN and H-GCN.

3.5. Electrochemical impedance studies

The resulted in EIS results measured at room temperature (25 ℃) were fitted by using suitable equivalent circuits (EC), which are shown in Fig. 5, to analyze the variations in impedance spectra for the uncoated and coated MS plates. Table 1 summarises the obtained EIS parameter. These models use the abbreviations Rs for the electrolytic resistance, Rf for film resistance, and Rct for charge transfer resistance. Additionally, constant phase elements (CPEdl and CPEf) were used to control how far away from the ideal capacitance the heterogeneous surface was. ZCPE ¼ [Y0 (jω)] might be used to indicate the value of CPE [21].

Because of its decreased resistance, GCN displays a smaller semicircle. Exfoliation increases the number of active sites and conductivity in the GCN by causing it to exhibit a resistance value (Rct) that is lower than that of bulk GCN. As a result, cell resistance is provided during the corrosion reaction while the charge transfer and hydrogen development are regulated. The H-GCN 3.5% NaCl electrolyte's Nyquist plot displays a larger semi-circular diameter than GCN, indicating higher corrosion resistance. As a result, it provides two separate loops: the

inductive loop occurs at a low frequency, and the capacitive loop appears at higher frequencies. Therefore, the current flow and resistance are improved during charge transfer [22]. In the case of 50 and 75 ℃ NaCl conditions, the same electrochemical reactions occurred. Some decrease in conductivity was noticed when the temperature of the electrolyte gradually increased.

The peak-to-peak separation value is established, and the redox current significantly increases when exfoliated H-GCN is utilized to change the GCN. The results were in line with the EIS. These results demonstrate that bulk GCN exfoliation increases the number of electrons exchanged between the electrode surface and the analyte, hence enhancing electro-catalytic activity. Additionally, the exfoliated GCN has a strong covalent bond between the atoms of nitrogen to carbon. The nitrogen atom, therefore, contributes to an increase in electrochemical activity.

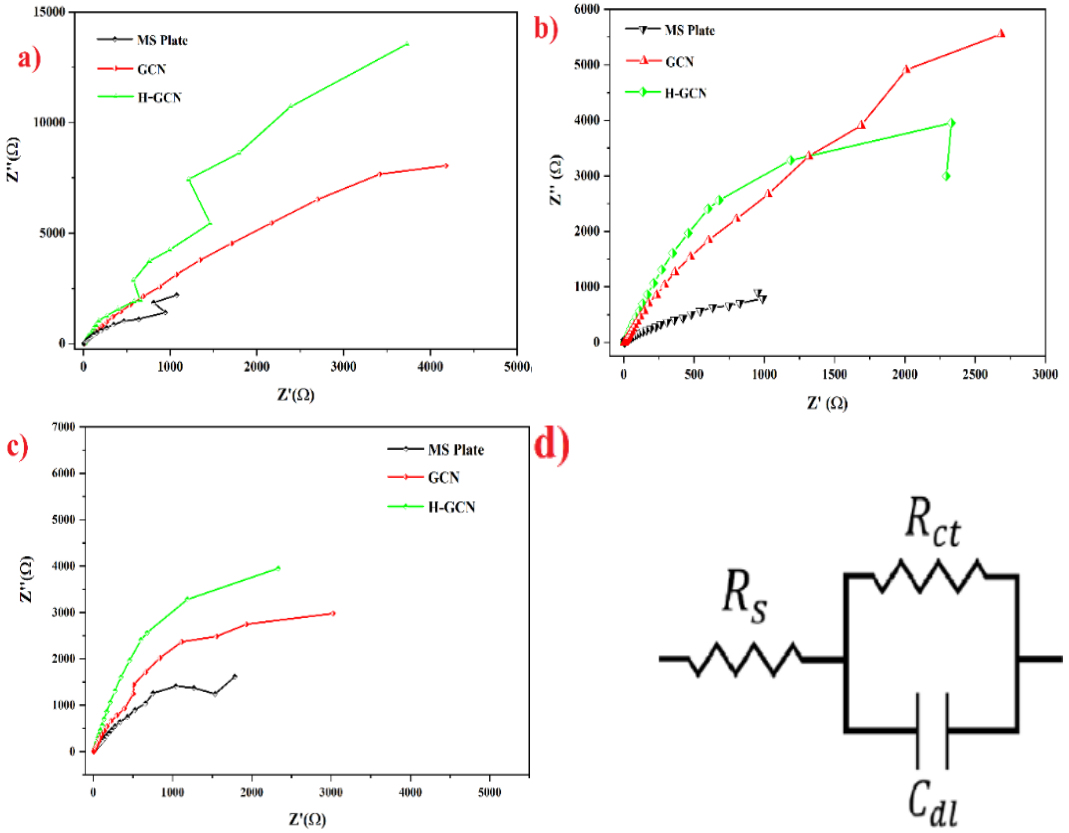

Fig. 5. Nyquist plot (a) and Equivalent circuit diagram (b) of uncoated MS plate and coated GCN and H-GCN after immersion in 3.5% NaCl medium.

Table 1. The electrochemical parameters of GCN and H-GCN obtained from EIS analysis.

Electrolyte Temperature	Sample	Rs (Ω)	Rp (Ω)	CPE
25 ℃	MS plate	104 k	1.04	154
	GCN	6.04	3.51	27.7 µ
	H-GCN	6.57	5.75	451 µ
50 ℃	MS plate	5.20	24.4	920 n
	GCN	6.21	30.4	149
	H-GCN	5.92	50.4	126
75 ℃	MS plate	5.62	21.4	392 µ
	GCN	5.20	24.4	920 n
	H-GCN	4.72	24.6	64.7

3.6. Potentiodynamic polarization study (Tafel plot)

Linear sweep voltammetry analysis has been observed to be increased with increasing temperature above room temperature, i.e., 50 ℃and 75 ℃. As shown in Figure 5, GCN and exfoliated H-GCN exhibit different potentiodynamic polarisation curves or Tafel plots in a 3.5% NaCl electrolytic solution at room temperature (25 ℃). As shown in Table 2, the electrochemical corrosion parameters were calculated using the Tafel plot.

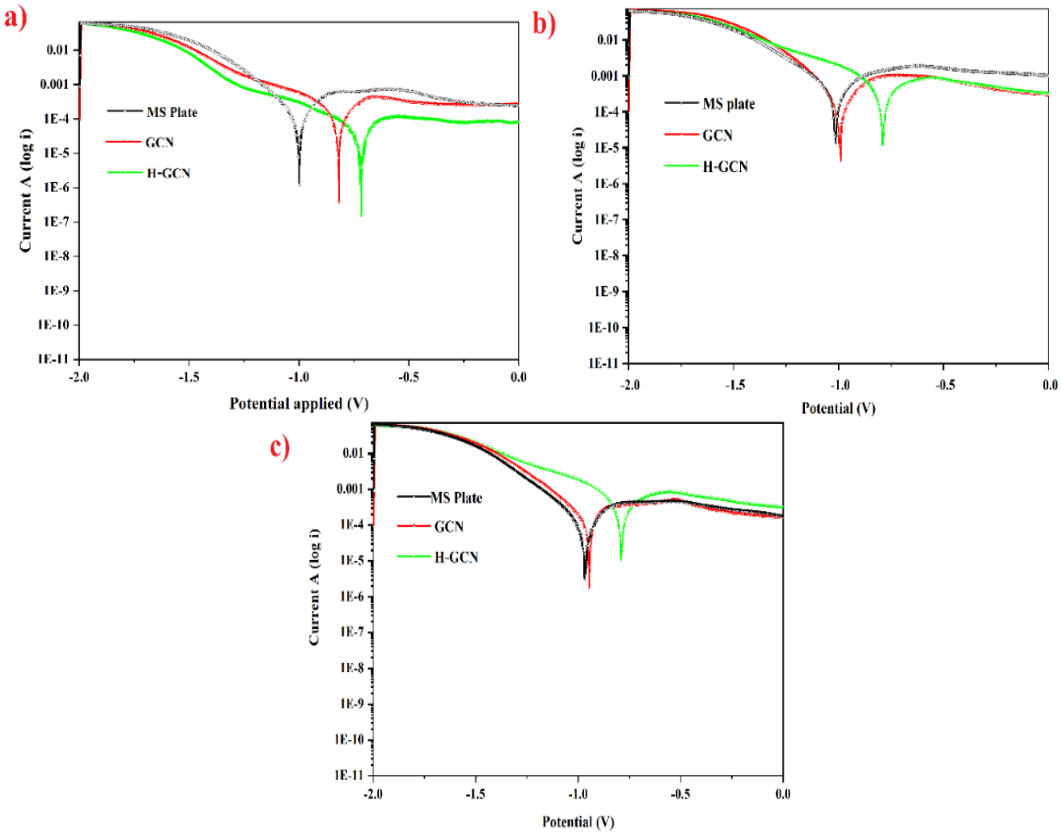

Fig. 5 Tafel plot for linear sweep voltammetry of uncoated and GCN and H-GCN-coated MS plates in NaCl electrolyte.

These parameters include the corrosion rate (CR), corrosion potential (Ecorr), corrosion current (Icorr), and polarisation resistance (Rp). Both coated MS plates have a higher corrosion resistance than untreated MS plates. The corrosion potential of the H-GCN is pushed towards a higher positive (anodic region) value for a 3.5% NaCl electrolytic medium than that of the GCN and uncoated MS plate.

This indicates that the coated GCN and H-GCN plates have a minimum corrosion rate (1.284 and 0.199 mm/year) than the untreated MS plate (3.215 mm/year). Thus, the above experimental observation confirmed that the hydrothermally exfoliated GCN over the MS plate and GCN showed they improve corrosion resistance in an aqueous NaCl electrolyte [23]. Therefore, hydrothermally exfoliated GCN showed a very minimal corrosion rate and strong electrochemical corrosion resistance (H-GCN) against GCN and MS plates. Additionally, for both GCN-coated MS plates and H-GCN-coated MS plates, corrosion rates and inhibition efficiency decrease as temperature increases. In the case of GCN-coated MS plates, corrosion rates and inhibition efficiency rise more quickly. A temperature range of 25 to 75 °C was found to be effective for GCN and H-GCN inhibitors. At the same time, corrosion resistance is comparably high when compared with the earlier reports [24-25]. The observed electrochemical impedance and linear sweep voltammetry analysis clearly reveals the prepared GCN and H-GCN could be a

potential candidate as corrosion inhibitor for radiator materials event through the temperature varies.

Table 3 presents a comparison of the corrosion inhibition behaviour of various metal surfaces coated with various metal oxide nanomaterials

Table 2. Tafel polarisation characteristics of GCN and H-GCN-coated MS plates in NaCl electrolyte and untreated MS plates.

Electrolyte Temperature	Sample	Icorr ($x10^{-4}$ A/cm^2)	Ecorr (V)	Polarisation resistance (Ω)	Corrosion rate	IE %
25 ℃	MS plate	2.766	-1.059	140.99	3.215	-
	GCN	1.105	-0.831	499.72	1.284	60.06
	H-GCN	0.171	-0.718	1491.3	0.199	93.81
50 ℃	MS plate	1.590	-1.0145	179.74	1.8483	-
	GCN	1.518	-0.78838	161.62	1.0998	40.49
	H-GCN	0.482	-0.9932	291.79	0.5611	86.79
75 ℃	MS plate	1.525	-0.8125	175.21	1.0989	-
	GCN	0.534	-0.9448	373.82	0.7216	47.34
	H-GCN	0.304	-0.9660	616.5	0.3539	67.82

Table 3. Compares the effectiveness of coating various metal surfaces with nanomaterials to increase corrosion inhibition behaviour.

S. No	Sample	Base metal	Electrolyte	Electrolyte Temperature	Inhibition efficiency (%)	Ref
1.	GCN	MS plate	3.5 % NaCl	25 ℃	60.1	This work
	H-GCN	MS plate	3.5 % NaCl	25 ℃	93.8	
2.	GCN	MS plate	3.5 % NaCl	50 ℃	40.49	
	H-GCN	MS plate	3.5 % NaCl	50 ℃	86.79	
3.	GCN	MS plate	3.5 % NaCl	75 ℃	47.34	
	H-GCN	MS plate	3.5 % NaCl	75 ℃	67.82	
4.	CuO	MS plate	3.5 % NaCl	25 ℃	53.5	22
5.	ZnO	Zn	3.5 % NaCl	25 ℃	50.1	23
6.	NiO	Zn	3.5 % NaCl	25 ℃	68.4	23
7.	NiO	Mg	3.5 % NaCl	25 ℃	61.1	25
8.	MnO_2	MS plate	1 M HCl	25 ℃	51.5	26

4. Conclusion

In conclusion, graphitic carbon nitride was exfoliated using a conventional hydrothermal method (GCN). The synthesized GCN was further characterized using physiochemical techniques. XRD results confirmed the synthesis of GCN by representing its strong peak, and FT-IR confirms the presence of a triazine ring during the thermal polymerization of urea. SEM images reveal spherical shape morphology in H-GCN synthesis. Additionally, the electro-catalytic activity increase was due to the H-GCN. GCN and H-GCN were prepared for the electrochemical method and applied over the MS plate surface to prevent corrosion in an aqueous NaCl electrolyte. According to electrochemical analyses of aqueous NaCl electrolytes, the corrosion rate in H-GCN has significantly decreased. The Nyquist plot further demonstrated the more excellent resistance to corrosion of H-GCN in NaCl electrolytes. Specifically, while increasing temperature, the mild steel plate corrosion rate gradually decreased for GCN and H-GCN samples.

References

[1] Yang, Guoqiang, Taijun Chen, Bo Feng, Jie Weng, Ke Duan, Jianxin Wang, Xiaobo Lu. Journal of Alloys and Compounds 770 (2019): 823-830; https://doi.org/10.1016/j.jallcom.2018.08.180

[2] Kavitha, V., P. Mahalingam, M. Jeyanthinath, and N. Sethupathi. Materials Today: Proceedings 23 (2020): 12-15; https://doi.org/10.1016/j.matpr.2019.05.351

[3] Gaddam, Sashivinay Kumar, Ramyakrishna Pothu, and Rajender Boddula. Polymer Composites 41, no. 2 (2020): 430-442; https://doi.org/10.1002/pc.25410

[4] Wang, Wenjun, Piao Xu, Ming Chen, Guangming Zeng, Chen Zhang, Chengyun Zhou, Yang Yang et al., ACS Sustainable Chemistry & Engineering 6, no. 11 (2018): 15503-15516; https://doi.org/10.1021/acssuschemeng.8b03965

[5] Kavitha, V., J. Mayandi, P. Mahalingam, and N. Sethupathi. Materials Today: Proceedings 35 (2021): 48-52; https://doi.org/10.1016/j.matpr.2019.05.437

[6] Kesavan, Ganesh, and Shen-Ming Chen, Diamond and Related Materials 108 (2020): 107975; https://doi.org/10.1016/j.diamond.2020.107975

[7] Kumar, A. Madhan, Abuzar Khan, Mohd Yusuf Khan, Rami K. Suleiman, Jobin Jose, and Hatim Dafalla, Materials Chemistry and Physics 251 (2020): 122987; https://doi.org/10.1016/j.matchemphys.2020.122987

[8] Sachith, B. M., S. Sandeep, S. Nandini, S. Nalini, C. S. Karthik, N. Kumara Swamy, P. Mallu, and J. G. Manjunath, Surfaces and Interfaces 20 (2020): 100603; https://doi.org/10.1016/j.surfin.2020.100603

[9] Mohammad, Akbar, Mohammad Ehtisham Khan, Md Rezaul Karim, Moo Hwan Cho, and Taeho Yoon, Ceramics International 47, no. 16 (2021): 23578-23589; https://doi.org/10.1016/j.ceramint.2021.05.076

[10] Vasudevan, D., D. Senthilkumar, and S. Surendhiran, International Journal of Thermophysics 41 (2020): 1-19; https://doi.org/10.1007/s10765-020-02651-6

[11] Roshni, C. P., K. Jithesh, M. Manuraj, K. Govind Raj, and R. B. Rakhi, Results in Chemistry 4 (2022): 100498; https://doi.org/10.1016/j.rechem.2022.100498

[12] Lu, Chao, and Xi Chen, ACS nano 15, no. 12 (2021): 18777-18793; https://doi.org/10.1021/acsnano.1c06454

[13] Brindha, R., SS Raja Ajith, M. Nandhini, M. Selvam, Kittitat Subannajui, Kittikhun Khotmungkhun, and K. Sakthipandi, Bulletin of Materials Science 42 (2019): 1-12; https://doi.org/10.1007/s12034-019-1907-0

[14] Qiu, Pengxiang, Huan Chen, Chenmin Xu, Ning Zhou, Fang Jiang, Xin Wang, and Yongsheng Fu, Journal of Materials Chemistry A 3, no. 48 (2015): 24237-24244; https://doi.org/10.1039/C5TA08406G

[15] Selvam, M., K. Saminathan, P. Siva, P. Saha, and V. Rajendran, Materials chemistry and physics 172 (2016): 129-136; https://doi.org/10.1016/j.matchemphys.2016.01.051

[16] Appaturi, Jimmy Nelson, Thiruchelvi Pulingam, Shalini Muniandy, Ignatius Julian Dinshaw, Leo Bey Fen, and Mohd Rafie Johan, Materials Chemistry and Physics 232 (2019): 493-505; https://doi.org/10.1016/j.matchemphys.2018.12.025

[17] Vasudevan, D., D. Senthil Kumar, A. Murugesan, and C. Vijayakumar, Bulletin of the Polish Academy of Sciences: Technical Sciences 3 (2020).

[18] Zhang, Junling, Zengwei Zhu, Junwei Di, Yumei Long, Weifeng Li, and Yifeng Tu. Electrochimica Acta 186 (2015): 192-200; https://doi.org/10.1016/j.electacta.2015.10.173

[19] Zhang, Hanqiang, Qitong Huang, Yihong Huang, Feiming Li, Wuxiang Zhang, Chan Wei, Jianhua Chen et al., Electrochimica Acta 142 (2014): 125-131; https://doi.org/10.1016/j.electacta.2014.07.094

[20] Zhang, Le-Sheng, Wei Li, Zhi-Min Cui, and Wei-Guo Song, The Journal of Physical Chemistry C 113, no. 48 (2009): 20594-20598; https://doi.org/10.1021/jp907989j

[21] Mandal, M., A. P. Moon, G. Deo, C. L. Mendis, and K. Mondal, Corrosion Science 78

(2014): 172-182; https://doi.org/10.1016/j.corsci.2013.09.012

[22] S. Surendhiran, V. Gowthambabu, A. Balamurugan, M. Sudha, V.B. Senthil Kumar, K.C. Suresh, Mater. Today: Proc. 47(4), 1011-1016 (2021); https://doi.org/10.1016/j.matpr.2021.05.515

[23] S. Ramamoorthy, S. Surendhiran, D. Senthil Kumar, G. Murugesan, M. Kalaiselvi, S. Kavisree, S. Muthulingam, and S. Murugesan, Journal of Materials Science: Materials in Electronics 33, no. 12 (2022): 9722-9731; https://doi.org/10.1007/s10854-022-07776-y

[24] Verma, Dakeshwar Kumar, and Fahmida Khan, Green Chemistry Letters and Reviews 9, no. 1 (2016): 52-60; https://doi.org/10.1080/17518253.2015.1137976

[25] M. Sudha, S. Surendhiran, V. Gowthambabu, A. Balamurugan, R. Anandarasu, Y.A. Syed Khadar, D. Vasudevan, J. Bio Tribo-Corro. 7, 60 (2021); https://doi.org/10.1007/s40735-021-00492-w

[26] Y.A. Syed Khadar, S. Surendhiran, V. Gowthambabu, S.Halimabi Alias ShakilaBanu, V. Devabharathi, A. Balamurugan, Mater. Today: Proc. 47(4), 889-893 (2021); https://doi.org/10.1016/j.matpr.2021.04.335